# 90-20115176 *In-situ* Neutron Diffraction Study on Work-hardening Behavior in a Ferrite-Martensite Dual Phase Steel

**Satoshi Morooka [1] Naoko Sato [2] Mayumi Ojima [3] Stefanus Harjo [4] Yoshitaka Adachi [5] Yo Tomota [6] Osamu Umezawa [1]**

*1) Yokohama National University, Depertment of Materials Science and Engineering*
*79-5 Tokiwadai, Hodagaya-ku Yokohama, Kanagawa 240-8501, Japan*
*2) Kyusyu University, Doctoral Student of Engineering*
*1-2-1 Sengen, Tsukuba, Ibaraki 305-0047, Japan*
*3) University of Tokyo, Depertment of Materials Science and Engineering*
*7-3-1 Hongo, Bunkyo-ku, Tokyo 113-8656, Japan*
*4) Japan Atomic Energy Agency, MLF/J-PARC*
*2-4 Shirakata Shirane, Tokai, Naka-gun, Ibaraki 319-1195, Japan*
*5) National Institute for Materials Science*
*1-2-1 Sengen, Tsukuba, Ibaraki 305-0047, Japan*
*6) Ibaraki University, Depertment of Science and Engineering*
*4-12-1 Nakanarusawa, Hitachi, Ibaraki, 316-8511, Japan*

Presented at the JSAE Annual Congress on May, 18 ,2011

**ABSTRACT**: Strength and work-hardening in steels have been discussed from the viewpoint of heterogeneous deformation. *In-situ* neutron diffraction techniques made clear that the misfit strains between grains accompanied with the grain-scaled internal stress (intergranular stress). In the dual phase steel, the intergranular stress was superposed on phase stress. Both long-range internal stress and short-range one like forest dislocation hardening may cause the resistance for dislocation motion in the steels.

**KEY WORDS**: **materials, high-strength steel sheet, test/evaluation** / Neutron diffraction, elastic strain analysis [D3]

## 1. INTRODUCTION

Microstructural design in steels is a key technology to provide a good balance of high strength and high ductility, where heterogeneous plastic deformation occurs. Plastic deformation of a steel starts at the most preferable site for dislocation motion, *i.e.*, the softest site. Hence, the misfit plastic strains are essentially yielded after the onset of local plastic flow, leading to the generation of internal stress distribution. The phase stress has evidently been measured by neutron diffraction technique for plastically deformed steels. To understand the tensile behavior of a two-phase alloy, Eshelby ellipsoidal theory[(1)] and Mori-Tanaka mean field concept[(2)] have been employed. It is therefore helpful to obtain the direct evidence of lattice strains, lattice rotation (texture) etc. of the constituents in a dual phase alloy *in-situ* during deformation, which has been realized by employing neutron diffraction for bulky average.

In case of single phase steel, grain to grain yielding occurs in the beginning of deformation because differently oriented grains have different yield strengths. The single phase polycrystalline material behaves as if it would be an extreme of composite material. The misfit strains between grains accompany the grain-scaled internal stress which is called intergranular stress. In a dual phase steel, this intergranular stress is superposed on phase stress[(3)]. Even in a single crystal, strong region like cell wall develops during plastic deformation resulting in the generation of internal stress[(4, 5)].

The resistance for dislocation motion in steels may therefore be summarized by the long range internal stress and short range one like forest dislocation hardening. It is believed that the former is corresponding to "athermal stress component" and the latter "thermal component".

In an engineering point of view, the balance of strength and ductility/toughness is very important. In order to obtain the uniform elongation in strengthened materials, increasing of work-hardening is a key issue.

Hence, this study aims to examine work-hardening behavior during tensile deformation of high strength and high ductility ferrite-martensite dual phase steels at relatively small strain focusing on stress partitioning between the ferrite and martensite and among ferrite grains or maretnsite packets (block) with different orientation, according to *in situ* neutron diffraction.

## 2. EXPERIMENTAL PROCEDURES

### 2.1. Experimental materials

The chemical compositions of a steel used in this studied were 0.15C, 0.10Si, 1.00Mn, 0.011P, 0.005S, 0.86Ni, 0.76Cr, 0.25Mo, 0.003t-Al in mass%. The specimens in the form of the cold-rolled steel plate with 1mm was prepared by aging at 737℃ and

775 ℃ for 1.8ks to obtain ferrite-martensite dual phase microstructure with different martensite volume fraction, which were named as 737-DP and 775-DP steels.

The microstructures of steels were observed by scanning electron microscopy (SEM) with KEYENCE VE-9800. The martensite volume fraction is 46.5 and 76.2vol.%, which was determined by the 3 dimension (3D) topological analysis[6]. The martensite carbon content is 0.33 and 0.2mass%C (ferrite carbon content calculated by thermo-calc.), which was determined by a mass balance calculation[7]. The gauge part of tensile test specimens was 4mm in width, 36mm in length, and 1mm in thickness. The tensile tests were performed at room temperature with a constant cross-head speed of 0.5mm/min and an initial strain rate of $2.3\times10^{-4}$/s.

The plate tensile test specimens for in-situ neutron diffraction experiments with a gauge length of 50mm, width of 5mm and thickness of 1mm were machined from the as-received treated plates. *In-situ* diffraction experiments during tensile deformation were carried out at room temperature using an engineering diffractometer "TAKUMI[8]" at the J-PARC/MLF (**Fig. 1**). The instrument is equipped with a 20kN tensile tester mounted on the diffractometer, with its loading axis 45 degrees turned to the incident beam. There are two detector banks, which measure time-resolved diffraction patterns at fixed horizontal scattering angles of ±90 degrees. Each {*hkl*} reflection in the diffraction pattern (**Fig. 2**) is generated by a distinct family of polycrystalline grains similarly oriented with respect to the load axis. The two detector banks thus measure diffraction patterns from grains oriented in axial and transverse geometry with respect to the applied tensile stress. The *in-situ* diffraction experiments during tensile testing were conducted using stress control, with counting times of approximately 240s. Stress diffraction measurements in crystalline materials are based on the precise measurement of the deviation of lattice spacing ($d_{hkl}$) of particularly oriented {*hkl*} crystallographic planes or lattice parameter obtained from average lattice spacing ($a_{ph.}$) deviation due to residual or applied stresses. The lattice strain ($\varepsilon_{hkl}$) and the average phase strain ($\varepsilon_{ph.}$) can be determined from the measured changes in the $d_{hkl}$ and $a_{ph.}$, respectively, according to equation (1):

$$\varepsilon_{hkl}=(d_{hkl} - d^0_{hkl})/ d^0_{hkl},\ \varepsilon_{ph.}=(a_{ph.} - a^0_{ph.})/ a^0_{ph.} \quad (1)$$

where $d^0_{hkl}$ and $a^0_{ph.}$ are the particular lattice spacing and lattice parameter in the stress-free sample, respectively. Individual reflections in the diffraction pattern (**Fig. 2**) from both detector banks were analyzed by multi-peak fitting[9] to determine the ferrite peak position and the martensite peak position, from which the elastic lattice strains ($\varepsilon_{hkl}$) during the tensile test were evaluated.

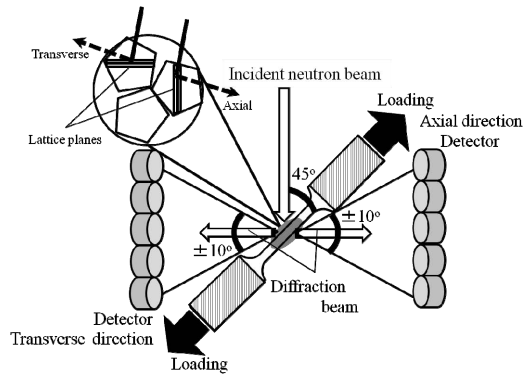


Fig. 1 Experimental configuration of the TAKUMI instrument on the beam line at J-PARC/MLF.

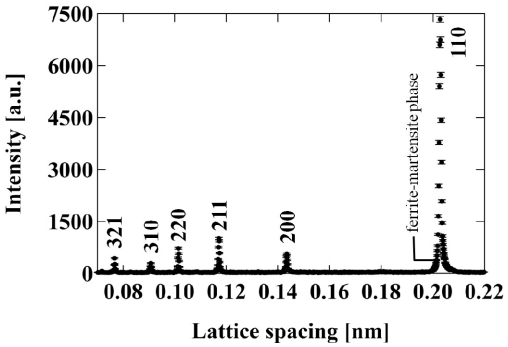


Fig. 2 An example of the full diffraction pattern of dual phase steel (737-DP steel).

**Fig. 3** displays the fitting results of overlopped (200) peaks along the axial direction (load direction) at 0 and 784MPa, respectively. As seen in inserted fitting curves for the ferrite and martensite, a single-peak fitting was not adequate and hence a multi-peak fitting was employed for the profiles analysis. To do such multi-peak fitting, firstly the mean carbon concentration of martensite was estimated from the mass balance calculation. As results, the carbon concentration was estimated to be and 0.33 and 0.2mass%C. Then, the *c/a* of bct martensite was postulated from equation (2)[10] to be 1.014 and 1.009, which was assumed not to change during tensile deformation.

$$c/a=1.000+0.045\times Xc\ (mass\%) \quad (2)$$

Probably, carbon concentration must differ from grain to grain. Hence, as a first approximation , the obtained diffraction peaks were fitted using two voigt curves with fixed *c/a* for martensite as try in **Fig. 3**. Similar separation technique for the ferrite and martensite or ferrite and bainite diffraction peak was successfully made for synchrotron X-ray and neutron diffraction of a dual phase steel by Cong *et al*[11, 12]. and Ohnuki *et al*[13]. , respectively. They have revealed the stress partitioning behavior

between the two similar crystal structure phases using such a proifile analysis. Obiously, the broadening peak comes from the martensite due to various crystal defects and the narrow one comes from the ferrite. Under a given applied stress, the martensite peak is more shfted, indicating the larger tensile stress in this phase. Such peak shifts with loading was examined for the other diffraction peaks of (110), (211), (220), and (310) for both of steels.

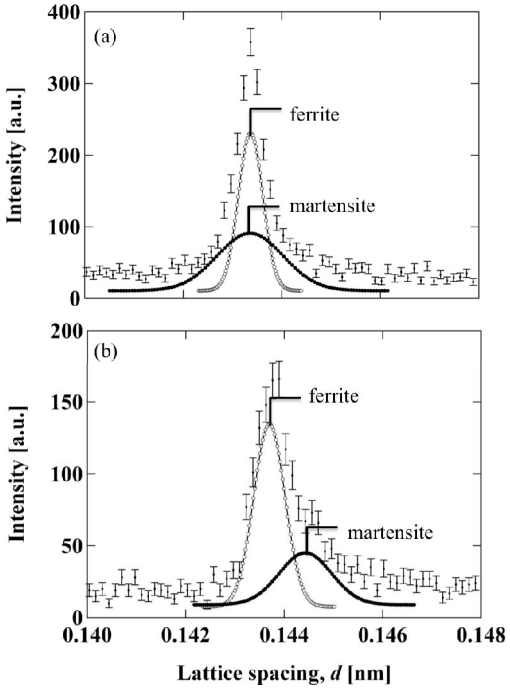


Fig. 3 (200) diffraction peaks for the ferrite and martensite phases at the applied stress (a) 0MPa and (b) 784MPa (737-DP）.

## 3. RESULTS AND DISSCSSION

### 3.1. Microstructure Characterization and mechanical properties

The structure characterization was performed with the aim to determine the ferrite and the martensite distribution homo-geneity and morphology across the specimens. **Fig. 4** shows the microstructures of the steel sheets. 737-DP and 775-DP steel are dual-phase types, of which the martensite volume fractions were 46.5 and 76.2 vol.%, respectively.

**Fig. 5** shows the nominal stress-strain curves of the two dual phase steels. As both dual phase steels were stored at room temperature before tensile straining, dislocation locking by segregation of solute carbon does not occur, and the occurrence of a yield point is suppressed. The 775-DP steel has a tensile strength of 915MPa which is about 80MPa above that of the 737-DP steel. Yield strength is higher, too. The higher strength levels are generally attributed to the higher phase fraction of the hard second phase. The uniform elongation is affected by the martensite volume fraction. **Fig. 6** shows the work-hardening rate as a function of true strain in both of steels. The initial work-hardening rate in both dual phase steels is very high. In particular, in the beginning, the 775-DP steel with high martensite volume fraction is higher than the 737-DP steel. However, when the plastic strain was increasing, work-hardening rate of 775-DP steel is lower than that of 737-DP steel.

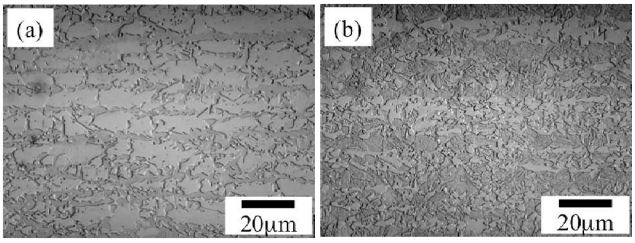


Fig. 4 Microstructure of the (a) 737-DP steel with the martensite volume fraction of 46.5vol.% and (b) 775-DP steel with the martensite volume fraction of 76.2vol.% produced by aging at 737℃ and 775℃ for 1.8ks.

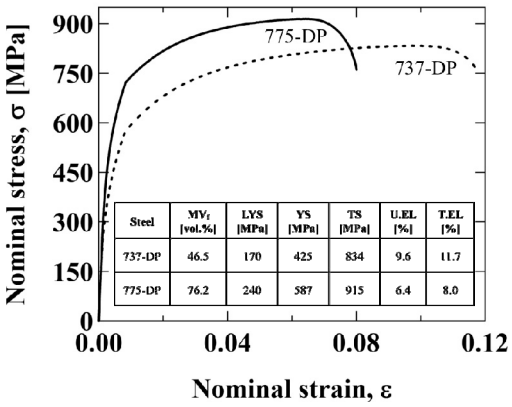


| Steel | $MV_f$ [vol.%] | LYS [MPa] | YS [MPa] | TS [MPa] | U.EL [%] | T.EL [%] |
|---|---|---|---|---|---|---|
| 737-DP | 46.5 | 170 | 425 | 834 | 9.6 | 11.7 |
| 775-DP | 76.2 | 240 | 587 | 915 | 6.4 | 8.0 |

Fig. 5 Nominal stress-strain curves of the steels with different martensite volume fraction. $MV_f$ : martensite volume furaction; LYS: low yield strength; YS: 0.2% proof stress; TS: tensile strength; U.EL: uniform elongation; T.EL: total elongation.

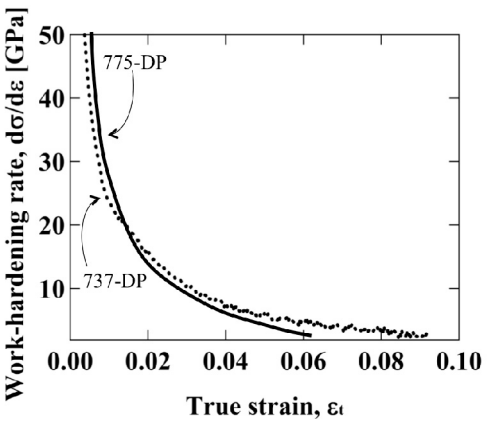


Fig. 6 Work-hardening rate as a function of true strain.

### 3.3. Stress partitioning among {*hkl*} family grains

The unique feature of the *in-situ* neutron diffraction experiment is that it provides information on the evolution of lattice strains and phase fraction in families of distinctly oriented grains during mechanical loading. The dependence on applied stress of lattice strains and intergrated intensities of individual reflections of the ferrite matrix and martensite are hereafter referred to as lattice plane responses. This allows us to follow the load partitioning not only between different phases but also between sets of similarly oriented grains. **Fig. 7** (a) and (b) show the evolution of lattice strains $\varepsilon_{hkl}$ of ferrite matrix family grains $\{110\}_f$, $\{200\}_f$ and $\{211\}_f$ and martensite family grains $\{110\}_m$, $\{200\}_m$ and $\{211\}_m$ during the tensile test on 737-DP steel in the axial direction. Throughout the following results and discussion, for the sake of simplicity and consistency, we will focus solely on the axial response (i.e. diffraction grains oriented similarly along the loading axis). As seen in **Fig. 7** (a), the slope is dependent on $\{hkl\}$ indicating different Young's modulus. The selected ferrite $\{hkl\}_f$ diffraction elastic modulus shows a good agreement with the prediction by Kröner model for a ferritic steel[14]. An indicated two arrows in **Fig. 7** (a), the deviation from linear elastic line takes plane earlier in [110] oriented family grains than [200]. This implies that [110] family grains are softer for plastic flow than [200] ones, leading to generation of intergranular stresses operating over a ferrite grain are formed with proceeding of deformation. When unloaded after tensile plastic deformation, all ferrite family grains are compressive. As seen in **Fig. 7** (b), all martensite $\{hkl\}_m$ were shown tensile residual elastic lattice strain in the axial direction. And $\{200\}_m$ residual elastic lattice strain was most of the highest in those strains. Therefore, martensite phase has different crystal orientation as well as ferrite matrix.

The difference in slopes of the *hkl* responses of both phases below the elastic limit is due to stress partitioning between grains controlled by the cubic elastic anisotropy factor $A_{hkl} = (h^2k^2 + h^2l^2 + k^2l^2) / (h^2 + k^2 + l^2)$[15, 16]. For cubic steel phases, the higher $A_{hkl}$ implies higher stiffness (diffraction elastic constant, $\varepsilon_{hkl}$) of <*hkl*> family grains aligned axially to the axial direction. Therefore, the axial stiffness of the selected family grain or ferrite matrix increases in the following order: $\{110\}_f$, $\{200\}_f$ and $\{211\}_f$, because A200<A110=A211. Similarly, the stiffness of martensite family grains $\{110\}_m$, $\{200\}_m$ and $\{211\}_m$ increases in the same order, because A200<A110=A211 This trend can be clearly seen in the ferrite matrix response to applied stress as well as in the martesnite resoponse.

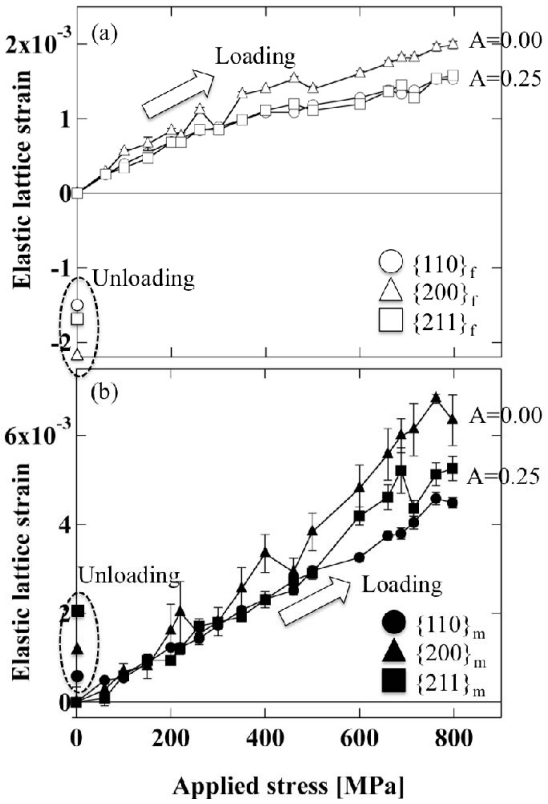


Fig. 7 Elastic lattice strains as a function of the applied stress: (a) selected ferrite reflections and (b) selected martensite reflections, during tensile deformation of DP-737 steel.

### 3.3. Stress partitioning between martensite (α') and ferrite (α) matrix

To make clear the stress partitioning among the constitute phases, the phase strain of each constitute was estimated by simply averaging two reflections {110} and {211} lattice strains. Because, the phase strain obtained using the Rietveld refinement is plotted at $A_{hkl} = 0.2$[17]. And hence, the evolutions of the average lattice strain (elastic phase strain) $\varepsilon_{ph.}$ of the ferrite matrix and martensite secondly phase during tensile tests on both of the investigated DP steels (737-DP and 775-DP) are plotted in **Fig. 8** as a function of the applied stress. As seen in **Fig. 8**, both ferrite and martensite strains in the axial direction increase with increasing of the applied stress linearly in the beginning. After the onset of plastic flow, i.e., yielding, elastic phase strain in ferrite pahse hardly changes or slightly increase with increasing of the applied stress. On the other hand, phase strain in martensite phase increases graetly with an increasing in the applied stress after the yielding. These results indicate good agreements with the predictions by a simple two-phase material model[18]; the strong martensite bears higher stress after the yielding, resulting in high work-hardening of the DP steel.

Let us try to draw a comparison between 737-DP and 775-DP steel about waor-hardening mechanisum. Fig. 9 shows phase

strains in the axial direction as a function of the applied strain. It is found that the elastic strain in martensite becomes higher with increaing of volume fraction compared at the same plastic strain level. This means that the load transfer takes place more effectively with increasing of volume fraction; in another words, plastic relaxation becomes more difficult. As seen Fig. 9, ferrite phase strain of 737-DP steel is lower than that of 775-DP steel. This indicates that martensite phase with large volume fraction hold to deformation of ferrite matrix. Thus, ferrite phase strain of 775-DP steel beared higher stress. And then, martensite phase strain of 737-DP steel is lower than that of 775-DP steel. Because, it must be effect of volume fraction and it may not almost be affect of martensite hardness.

Therefore, the work-hardening takes place more effectively with higher internal stress and larger volume fraction.

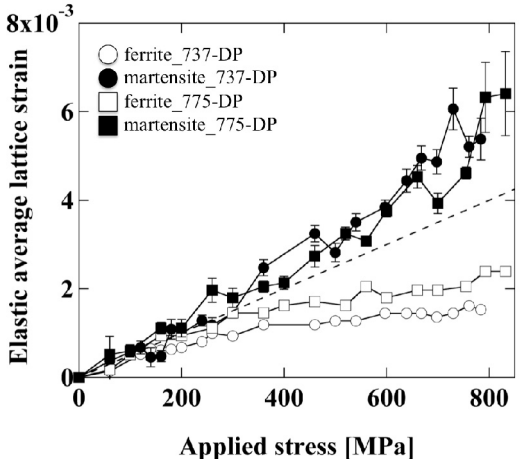


Fig. 8 Change in elastic average lattice strains (phase strains) as a function of the applied stress, indicated stress partitioning between ferrite and martensite on both of the investigated DP steels (737-DP and 775-DP).

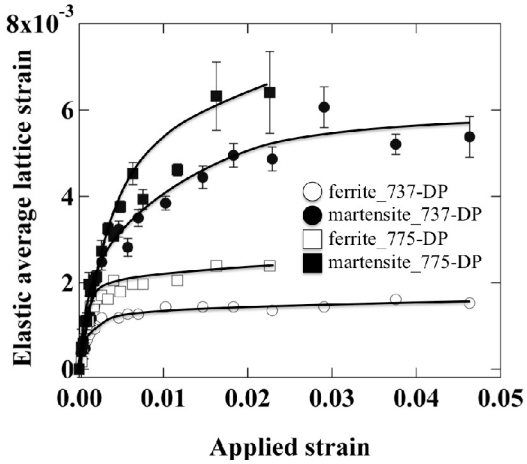


Fig. 9 Elastic average lattice strain versus overall plastic strain relationships re-plotted from Fig. 8.

## 4. SUMMARY

Tenisle behavior of the ferrite-martensite dual phase steels was studied under *in-situ* neutron diffraction. The origin of work-hardening behavior was discussed in this paper, leading to the following summary.

1) The misfit strains between grains accompany the grain-scaled internal stress which is called intergranular stress. This internal stress also has affected to the work-hardening behavior.

2) The misfit strains between phases accompany the phase-scaled internal stress which is called phase stress. This internal stress also has affected to the work-hardening behavior.

3) The work-hardening takes place more effectively with higher internal stress and larger volume fraction.

## ACKNOWLEDGMENTS

This series of investigation has been carried out with thoughtful assistance by an instrument scientists at neutron research facility (J-PARC). The authors highly appreciated useful discussion at the member meeting of the ISIJ research group (work-hardening properties and microstructures, leader of Prof. Higashida) .

## REFERENCES

(1) J. D. Eshelby: Proc. Rov. Sot., 1957, A241, p.376.

(2) T. Mori and K. Tanaka: Acta metall., 1973, 21, p.171.

(3) S. Morooka, Y. Tomota and T. Kamiyama: ISIJ Int., 2008, 48, p.525.

(4) H. Mughrabi: Phil. Mag., 2006, 86, p.4037.

(5) H. Mughrabi: Acta mater., 2006, 54, p.3247.

(6) N.Sato, M.Ojima. S.Morooka, Y.Tomota, Y.Adachi: Proc. of the 7th International conference on advanced materials (THERMEC'2011), Trans Tech Publications, Switzerland, 2012, in press.

(7) M. Calcagnotto, Y. Adachi, D. Ponge, D. Raabe: Acta Mater., 2011, 59, p.658.

(8) S. Harjo, K. Aizawa, T. Ito, H. Arima, J. Abe, A. Moriai, K. Sakasai, T. Nakamura, T. Nakatani, T. Iwahashi, T. Kamiyama: Mater. Sci. Forum, 2010, 652, p.99.

(9) T. Ohunuki, K. Asoo, Y. Tomota, S. Harjo: Tetsu-to-Hagane, 2011, 97, p.45.

(10) Z. Nisizawa: Martensite transformation, Muruzen, Tokyo, 1971, 1, pp.13-14.

(11) Z. H. Cong, N, Jia, X. Sun, Y. Ren, J.Almer and Y. D. Wang: Metall. Mater. Trans. A, 2009, A40, pp.1383-1387.

(12) N. Jia, Z. H. Cong, X. Sun, S. Cheng, Z. H. Nie, Y. Ren, P. K. Liaw and Y. D. Wang: Acta Mater., 2009, 57, p.3965.
(13) H. Ohnuki, K. Asoo, Y. Tomota and S. Harjo: Tetsu-To-Hagane, 2011, 97, pp.209-211.
(14) E. Kröner: Zeitschrift fur Physik, 1958, 151, pp.504-518.
(15) M. E. Fitzpatrick and A. Lodini: Analysis of Residual Stress by Diffraction using Neutron and Synchrotron Radiation, Taylor & Francis, 2003, pp.47-59.
(16) T.Shinozaki, S.Morooka, T.Suzuki, Y.Tomota and T.Kamiyama: Proc. of the 3rd International Conference on Advanced Structural Steels (ICASS 2006), NIMS, 2006, pp.22-24.
(17) F. Bollemath, V. Hank and E. Z. Muller: Metallkd, 1967, 58, pp.76-82.
(18) Y.Tomota, S.Morooka, K.Ikeda, M.Ojima, S.Harjo and Y.Adachi: Proc. of the 2nd International Symposium on Steel Science (ISSS 2009), ISIJ, 2009, pp.27-37.